Site Segregation in Small Rhodium Bimetallic Aggregates: A Combined Catalytic and Quantum Chemical Study

Bernard Coq,*,† Annick Goursot,*,† Touria Tazi,† Francois Figuêras,† and Dennis R. Salahub‡

Contribution from the Laboratoire de Chimie Organique Physique et Cinêtique Chimique Appliquêes, URA 418 CNRS, ENSCM, 8 rue Ecole Normale, 34053 Montpellier Cedex 1, France, and the Dêpartement de Chimie, Universitê de Montrêal, Case Postale 6128, Succursale A, Montrêal, Quêbec, H3C 3J7 Canada. *Received July 24, 1990*

Abstract: The spatial distribution of the two components at the surface of small bimetallic aggregates has been investigated by using the hydrogenolysis of model alkanes and quantum chemical calculations. The catalysts were supported on γ-alumina and consisted of rhodium particles (size $\simeq$ 1-2 nm), modified by Sn, Pb, Sb, or Ge. They were prepared by using the surface reaction of rhodium hydride with organometallic compounds. On pure Rh catalysts, the conversions of *n*-hexane and methylcyclopentane show a low sensitivity to changes of the surface topology, corresponding either to a modification of the particle size or to the addition of a small amount of Sn or Ge modifier. At variance, the hydrogenolysis of 2,2,3,3-tetramethylbutane is highly sensitive to the topology of the surface and yields selectively 2,2,3-trimethylbutane and methane on small particles, which have mainly sites of low coordination (corners and edges), whereas isobutane is selectively formed on large particles, which show more sites of high coordination (facets, planes). The addition of a small amount of Sn or Pb favors the formation of isobutane, but the addition of an equivalent amount of Ge promotes demethylation. Therefore, Sn and Pb inhibit selectively the reactions catalyzed by the sites of low coordination, and this demonstrates that there is a topological segregation to these sites, while Ge atoms appear to be randomly distributed at the surface. Quantum chemical calculations of the relative stabilities of $Rh_{10}M_4$, $Rh_{10}M_3$, and $Rh_{12}M$ model clusters (M = Sn, Ge), with different geometries and different localizations of M, support the conclusion that the most stable aggregates are those where the M atoms are localized at the periphery. However, Sn atoms are shown to segregate essentially to the corner sites, whereas Ge atoms do not have as definite a preference. Moreover, Ge differs from Sn in the sense that Ge atoms tend to disperse in the Rh lattice, while Sn atoms tend to form Sn-Sn bonds.

Introduction

Multimetallic formulations are currently used to improve the properties of metal catalysts. Over the last decades the addition of Sn, Re, and Ir to Pt has led to new generations of reforming catalysts with better selectivity for isomerization and aromatization, and a longer lifetime on stream.[1] Similarly, the upgrading of C_2, C_3, and C_4 olefin cuts for polymerization was improved by adding a second component (Cu, Au, Pb) to Pd-based catalysts.[2] Finally the search for higher selectivities for producing fine chemicals opened up a new field of applications.

For both technical and academic reasons the way by which the second component modifies the properties of pure metals is a subject of interest, and it is still not well-elucidated. Depending on the reaction and the operating conditions considered, geometrical and/or electronic effects were claimed (see ref 1 for a review). In any case, understanding the bimetallic effect would require the best possible knowledge for the following questions: (i) Are the two elements intimately interacting in the same aggregates? (ii) Does surface segregation of one component occur? (iii) Are the two elements randomly distributed in the surface layer or not?

The first point is not totally fulfilled when bimetallic catalysts are prepared by classical means. Successive or co-impregnation of the carrier with aqueous solutions of salts of the two metals and subsequent thermal treatments have led to a wide variety of aggregate compositions, which was well evidenced in the case of PtSn catalysts for instance.[3,4] A new way for obtaining bimetallic particles, from organometallic precursors, was recently claimed[5] and successfully applied for the preparation of Pt, Pd, Rh, Ru, and Ni with a wide variety of second components including Sn, Pb, Sb, Ge, and Si.[6,7] The highly selective interaction between a metal alkyl, e.g. $Sn(C_4H_9)_4$, and the metal particles of a parent material, e.g. Rh/Al_2O_3, led to a well-tailored $RhSn/Al_2O_3$ bimetallic catalyst. Furthermore, preparing bimetallic catalysts by this method allows the obtention of various formulations, starting from the same parent monometallic catalyst, either by varying the amount of the second component or by changing the nature of this component but with the same bulk composition. The bimetallic effect was thus well-studied in different reactions including the following: hydrogenolysis of ethyl acetate to ethanol on $RhSn/SiO_2$,[8] hydrogenation of isoprene and 2-methyl-1-buten-3-yne on PdM/Al_2O_3 (M = Sn, Pb, Sb, Ge),[9] alkane hydrogenolysis on RuM/Al_2O_3,[10] and conversion of *n*-hexane on $PtSn/Al_2O_3$.[11]

The second question to be asked is about the surface composition in bimetallic particles. The occurrence of segregation of one component of an alloy to the surface is now well-established, as well as its influence on the catalytic properties (see ref 1). Two theoretical models account for surface enrichment in alloys. First, the broken-bond model predicts segregation to the surface of the component possessing the lowest heat of sublimation.[12] Second, the size difference model proposes enrichment of the surface by the component of larger atomic volume.[13] When going from bulk alloys to small supported bimetallic particles the occurrence of surface segregation remains in many cases, as evidenced by EXAFS studies.[14,15]

* Authors to whom correspondence should be addressed.
† Laboratoire de Chimie Organique Physique et Cinêtique Chimique Appliquêes.
‡ Universitê de Montrêal.

(1) Clarke, J. K. A.; Creaner, A. C. M. *Ind. Chem. Prod. Res. Dev.* **1981**, *20*, 574. Ponec, V. *Advances in Catalysis*; Academic Press: London and New York, 1983; Vol. 32, p 149.
(2) Boitiaux, J. P.; Cosyns, J.; Derrien, M.; Leger, G. *Hydrocarbon Processing* **1985**, *March*, 51.
(3) Bacaud, R.; Bussiere, P.; Figueras, F. *J. Catal.* **1981**, *69*, 399.
(4) Burch, R. *J. Catal.* **1981**, *71*, 348.
(5) Travers, C.; Chan, T. D.; Snappes, R.; Bournonville, J. P. U.S. Patent 4,456,775, 1984.
(6) Margitfalvi, J.; Hegedüs, M.; Göbölös, S.; Kern Talas, E.; Szedlacsek, P.; Szabo, S.; Nagy, F. *Proceedings 8th International Congress on Catalysis*, Berlin, 1984; Verlag Chemie: Weinheim, 1984; Vol. 4, p 903. Travers, C.; Bournonville, J. P.; Martino, G. *Ibid.*, Vol. 4, p 891.
(7) Aduriz, H. G.; Bodnariuk, P.; Coq, B.; Figueras, F. *J. Catal.* **1989**, *119*, 97.
(8) Candy, J. P.; El Mansour, A.; Ferretti, O. A.; Mabilon, G.; Bournonville, J. P.; Basset, J. M.; Martino, G. *J. Catal.* **1988**, *112*, 210.
(9) Aduriz, H. G.; Bodnariuk, P.; Coq, B.; Figueras, F. *J. Catal.* In press.
(10) Coq, B.; Bittar, A.; Dutartre, R.; Figueras, F. *J. Catal.* In press.
(11) Margitfalvi, J.; Szabo, S.; Nagy, F. *Stud. Surf. Sci. Catal.* **1986**, *27*, 373.
(12) Williams, F. L.; Nason, D. *Surf. Sci.* **1974**, *45*, 377.
(13) McLean, D. In *Grain Boundaries in Metals*; Clarendon Press: Oxford, 1957.

0002-7863/91/1513-1485$02.50/0

However, on small particles (1–2 nm) surface atoms tend to represent the majority of the atoms of the particle and the surface enrichment loses meaning. Nevertheless, on these small aggregates the surface contains sites of different topologies: low index planes, kinks, edges, corners, etc. The distribution of the different components of the bimetallic particles could be ordered, and one component would occupy sites of a given topology preferentially.[16] This concept was formulated early on by Burton et al. and Sundaram and Wynblatt,[17] using different theoretical approaches. Recently this concept was rejuvenated in a study by Strolh and King.[18] These authors modeled perfect cubooctahedral bimetallic particles with a Monte-Carlo simulation technique that uses a coordination-dependent potential model. For the Pt–Ib system (Ib = Cu, Ag, Au) and particles in the 2–6 nm range, the authors reached the conclusion that the Ib element not only accumulated at the surface layer but subsequently segregated to low coordination sites (edges and corners). The extent of this site segregation depends on both the cluster size and the nature of the Ib element. Unfortunately, experimental evidence for this phenomenon is lacking, and spectroscopic techniques like EXAFS do not appear accurate enough to validate these concepts so far.

For several years our group has been developing the use of surface reactions as probes for delineating changes of microstructure in supported bimetallic particles.[19] This approach parallels that of Gault's group in Stasbourg, who studied Pt-based catalysts during the seventies. The change of catalytic properties, activity and selectivity, for alkane conversion over rhodium is related to the occurrence of surface complexes[20,21] differing according to the particle size and the nature of the alkane.[22] In this respect, the conversion of 2,2,3,3-tetramethylbutane (TeMB) appears highly sensitive to changes of surface topology on small Rh and Ru particles.[19]

The main features of TeMB hydrogenolysis on Rh/Al_2O_3 are the following: (1) On large particles (>3 nm), with a high proportion of atoms in low-index planes (coordination number N = 8, 9), TeMB is selectively split into isobutane (iC_4 > 96%). This central cleavage of TeMB between the two quaternary carbon atoms appears as a more general rule on poorly dispersed metals, since it readily occurs on Pt, Ni, and Ru too.[23] (2) On very small particles (<1 nm), exhibiting essentially edges and corners (*N* = 5, 6), TeMB is selectively split into CH_4 and 2,2,3-trimethylbutane (iC_4 < 4%).

These behaviors reflect the formation of different surface intermediates, $\alpha\gamma$ and $\alpha\delta$, which have been postulated also for the $TeMB/D_2$ exchange.[21] For the reactions of TeMB on Rh, the activation energy for exchange is 20 kcal/mol,[20,21] whereas it is 50–60 kcal/mol for hydrogenolysis.[22] It then can be supposed that the slow step of the reaction is the decomposition of the surface complex. In organometallic chemistry, the stoichiometric reaction of metallacyclopentanes has been shown by Grubbs et al.[24] to depend on the coordination of the metallic complex, the central C–C bond splitting being observed for high coordination. An interpretation of the reactivities of these complexes has been proposed by McKinney et al.[25] in terms of orbital symmetry.

Table I. Main Features for the Preparation and Hydrogen Chemisorption of Rh/Al_2O_3 Catalysts

catalysts	wt % Rh	liquid/solid,[a] mL/g	reduction step: temp, K	reduction step: duration, h^{-1}	reduction step: gas	H/Rh
RAl5[b]	2.0	7	1173	48	$H_2 + H_2O$[e]	0.07
RAl3[b]	2.6	2	973	48	$H_2 + H_2O$[e]	0.35
RAl8[c]	1.32	5	773	4	H_2	0.74
RAl6[c]	1.16	5	773	4	H_2	0.90
RAl2[c,d]	0.6	5	773	4	$H_2 + N_2$[f]	1.4
RAl2D[c,d]	0.45	2.5	773	4	$H_2 + N_2$[f]	1.7

[a] Ratio between $Rh(acac)_3$ solution and γ-Al_2O_3 during the contacting step. [b] $Rh(acac)_3$ in trichloroethylene solution. [c] $Rh(acac)_3$ in toluene solution. [d] Exchanged and calcined samples. [e] H_2/H_2O (97.5/2.5 (v/v)). [f] H_2/N_2 (20/80 (v/v)).

Nickelacyclopentane degradation to form ethylene is symmetry forbidden for a square-planar complex, whereas it is allowed for tetrahedral Ni coordination. Those authors proposed a distorted tetrahedral structure, formed in going from a penta- to a tetracoordinated complex, as the source of ethylene (central C–C bond cleavage). A recent study using local spin density functional theory[26] has shown that, besides a tetrahedral triplet state, this compound has three low-lying singlet states, related to different electronic configurations. Depending on the steric hindrance of the two external ligands (opposite to the metallacycle), cyclobutane formation could, in principle, be consistent with two of them, the square-planar complex and the less distorted tetrahedral form, while ethylene formation could proceed from the most distorted tetrahedral species. Of course, the possibilities for geometric distortion around a specific metal atom are fewer in an aggregate than in an organometallic system. However, these studies suggest that the geometry around the metal active site plays a preponderant role in the degradation of the surface intermediate.

A similar reasoning may be applied to the catalytic problem of the preferred formation of isobutane on large particles. The conversion of TeMB is then a sensitive probe for the coordination of the surface atoms.

This approach has been applied previously with success for the study of $RhCu/SiO_2$[27] and RuM/Al_2O_3[10] bimetallic catalysts, which showed that Cu in RhCu and M = Sn, Pb, Sb in RuM particles segregate into low coordination sites, while Ge is more randomly distributed on the surface layer of RuGe particles. In this work, we extend the same methodology to RhM/Al_2O_3 catalysts (M = Sn, Pb, Sb, Ge), using the conversion under hydrogen of *n*-hexane, methylcyclopentane, and TeMB. Moreover, site segregation in bimetallic catalysts being a fundamental problem, we found it valuable to use a combined experimental and theoretical approach in the present case of RhM aggregates. The theoretical study has been performed with use of the LCGTO-MP-LSD method,[28,29] which has provided reliable results involving transition-metal clusters. As we found previously that RuSn and RuGe have opposite behaviors we have chosen to compare the possible segregation of Sn and Ge in RhM aggregates by comparing the relative stabilities of cluster models containing Sn and Ge at different coordination sites. Two models of 14 and 13 atoms have been used to represent the (100) and (111) faces, respectively. They have been chosen to fulfill the following requirements: (i) nearest neighbors of a specific site be present; (ii) different sites be compared on clusters containing the same number of Rh and Sn(Ge) atoms.

Experimental Section

Reactants. Hydrogen of high purity grade (99.99%) was used for the catalytic experiments, and hydrogen of ultra-high purity (99.9995%) was

(14) Sinfelt, J. H.; Via, G. H.; Lytle, F. W. *J. Chem. Phys.* **1980**, *72*, 4832; **1982**, *76*, 2279. Meitzner, G.; Via, G. H.; Lytle, F. W.; Sinfelt, J. H. *J. Chem. Phys.* **1983**, *78*, 2533.
(15) Van't Blick, D. C.; Koningsberger, D. C.; Prins, R. *J. Catal.* **1986**, *97*, 210.
(16) Balseiro, C. A.; Moran-Lopez, J. L. *Surf. Sci.* **1985**, *156*, 404.
(17) Burton, J. J.; Hyman, E.; Fedak, D. G. *J. Catal.* **1975**, *37*, 106. Sundaram, V. S.; Wynblatt, P. *Surf. Sci.* **1975**, *52*, 569.
(18) Strohl, J. K.; King, T. S. *J. Catal.* **1989**, *116*, 540.
(19) Coq, B.; Bittar, A.; Tazi, T.; Figueras, F. *J. Mol. Catal.* **1989**, *55*, 34.
(20) Cogen, J. M.; Maier, W. F. *J. Am. Chem. Soc.* **1986**, *108*, 7752.
(21) Kemball, C.; Brown, R. *J. Chem. Soc., Chem. Commun.* **1987**, 771. Brown, R.; Kemball, C.; Sadler, I. H. *Proceedings of the 9th International Congress on Catalysis*, Calgary, 1988; Chemical Institute of Canada: Ottawa, 1988; Vol. 3, p 1013.
(22) Coq, B.; Figueras, F. *J. Mol. Catal.* **1987**, *40*, 93.
(23) Zimmer, H.; Tetenyi, P.; Paal, Z. *J. Chem. Soc., Faraday Trans. 1* **1982**, *78*, 3573. Coq, B.; Bittar, A.; Figueras, F. *Appl. Catal.* **1990**, *59*, 103.
(24) Grubbs, R. H.; Miyashita, A. *J. Am. Chem. Soc.* **1978**, *100*, 1300.
(25) McKinney, R. J.; Thorn, D. L.; Hoffmann, R.; Stockis, A. *J. Am. Chem. Soc.* **1981**, *103*, 2595.
(26) Peluso, A.; Salahub, D. R.; Goursot, A. *Inorg. Chem.* **1990**, *29*, 1544.
(27) Coq, B.; Dutartre, R.; Figueras, F.; Rouco, A. *J. Phys. Chem.* **1989**, *93*, 4904.
(28) Andzelm, J.; Radzio, E.; Salahub, D. R. *J. Chem. Phys.* **1985**, *83*, 4573.
(29) Salahub, D. R. *Applied Quantum Chemistry*; Smith, V. H., Jr., Schaefer, H. F., III, Morokuma, K., Jr., Eds.; Reidel: Dordrecht, 1986, p 185. Salahub, D. R. *Adv. Chem. Phys.* **1987**, *69*, 447.

Table II. Main Characteristics of RhM/Al_2O_3 Catalysts (M = Sn, Pb, Ge, Sb)

catalysts	M/Rh (at/at)	H/Rh	TON, h^{-1} nH	TeMB	MCP
RAl2	0	1.4	249	65	100
RAl2Sn2	0.21	1.5	80	2.1	32
RAl2Sn3	0.50	1.2	4.0	0.62	16
RAl6	0	0.9	98	7.6	192
RAl6Sn1	0.24	0.43	80	7.2	230
RAl6Sn2	0.43	0.39	46	3.3	116
RAl6Sn3	0.75	0.16	0.30	0.02	0.76
RAl6Sn4	1.6	0.11	0.015		0.004
RAl8Pb1	0.73	0.05	2.0	0.1	19.5
RAl8Pb2	0.19	0.40	100	10.2	275
RAl8Pb3	0.37	0.27	30	4.0	185
RAl8Ge1	0.20	0.24	9.4	0.2	19
RAl8Ge2	0.70	0.11	6.1	0.08	14
RAl8Sb	0.19	0.51	160	37	310

used for adsorption measurements. The hydrocarbons used were *n*-hexane (nH, Fluka, purity >99.6%), methylcyclopentane (MCP, Aldrich, purity >99.63%), and 2,2,3,3-tetramethylbutane (TeMB, Aldrich, purity >99.99%). Rhodium acetylacetonate ($Rh(acac)_3$, Aldrich, purity >97%) was used as precursor for the catalysts. This precursor was chosen in order to avoid the effect of chlorine which could affect the chemisorption or catalytic properties.[30-32] The precursor was dissolved either in dehydrated toluene or in trichloroethylene (purities >99.5%).

The second metal was introduced as tetra-*n*-butyltin (Merck, purity >95%), tetra-*n*-butyllead (Alfa, purity >98%), tetra-*n*-butylgermanium (Alfa), and tri-*n*-butylantimony (Alfa). These organometallic compounds were dissolved in *n*-heptane (Fluka, purity >99%). The carrier was γ-alumina from Woelm (surface area 200 m^2/g).

Preparation of Monometallic Rhodium Catalysts. The Rh/Al_2O_3 samples were prepared by ligand exchange of $Rh(acac)_3$. The requisite amount of $Rh(acac)_3$ was dissolved in toluene, or trichloroethylene, and then contacted with γ-Al_2O_3 at room temperature for several hours. Afterwards, the solution was either evaporated or filtered. These solids were dried at 298 K under vacuum. Some catalysts were then subjected to a calcination step under air at 673 K for 4 h. Finally, all the samples were reduced under varying conditions. The precisions required for preparing catalysts according to these protocols are given in Table I.

Preparation of Bimetallic Rhodium Catalysts. The bimetallic RhM/Al_2O_3 samples (M = Sn, Pb, Ge, Sb) were prepared by contacting in situ, and under bubbling hydrogen, a prereduced Rh/Al_2O_3 parent catalyst with the desired amount of $(C_4H_9)_4Sn$, for instance, in *n*-heptane solution. The controlled surface reaction was carried out under hydrogen atmosphere at 363 K, with a solid/liquid ratio of 1 g/10 cm^3. The formal reaction is

$$(C_4H_9)_4Sn + Rh/Al_2O_3 \xrightarrow{H_2} RhSn(C_4H_9)x/Al_2O_3 + (4-x)C_4H_{10}$$

These solids were then dried under vacuum at room temperature and reduced subsequently under hydrogen at 673 K for 4 h. True bimetallic particles were thus obtained.

Characterization. The chemisorption of hydrogen was carried out in a conventional volumetric apparatus, at 298 K in the 0–20 kPa pressure range. The sample was first reactivated in situ under flowing hydrogen at 673 K overnight and then evacuated to 1.2 10^{-4} Pa, at the same temperature, for 3 h; hydrogen was then adsorbed. The linear part of the isotherm, usually between 10 and 20 kPa, was extrapolated to zero pressure to determine the hydrogen uptake. On highly dispersed samples, with particle sizes below 1 nm, the stoichiometry of hydrogen adsorption reached values higher than unity. It was reported recently that the stoichiometry of hydrogen adsorption changes with Rh particle size and is larger than unity on small particles.[33] This introduces an uncertainty for the number of surface Rh atoms, which can reach 30% on well-dispersed samples. It must then be realized that small changes of catalytic activity have little significance; changes of selectivity thus appear to have a higher reliability to characterize a catalyst. The size of the metallic particles was checked by transmission electron microscopy with a JEOL 100CX microscope. The agreement with chemisorption is generally good.

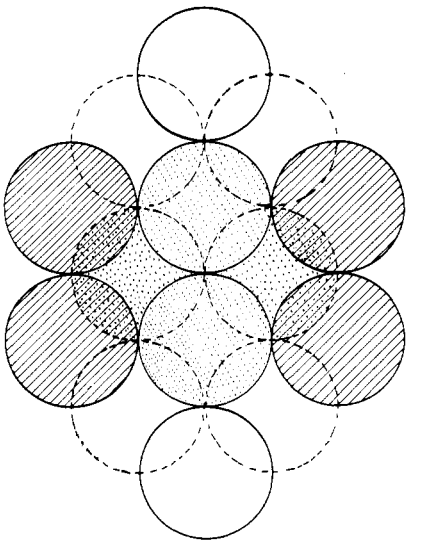

Figure 1. Model cluster of the (100) face of $Rh_{10}M_4$: solid line, 1st layer; dashed line, 2nd layer; hachered spheres, Sn and Ge atoms in low coordinated sites ($N = 4$); dotted spheres, Sn and Ge atoms in high coordination sites ($N = 8$).

Chemical compositions of the solids were determined by elemental analysis after dissolution, at the Service Central d'Analyse (CNRS, Solaize, France).

Tables I and II summarize the main characteristics of the catalysts.

Catalytic Tests. The reactions of *n*-hexane, methylcyclopentane, and 2,2,3,3-tetramethylbutane with hydrogen were carried out at atmospheric pressure in a microflow reactor. The effluents were analyzed by sampling on line to a gas chromatograph equipped with a J&W capillary column (30 m × 0.5 mm i.d., DB1 apolar bonded phase). An aliquot (50–100 mg) of the sample used for chemisorption measurements was reactivated in situ under flowing hydrogen at 673 K overnight. The reaction temperatures ranged from 463 to 508 K, and the molar ratios of reactants were the following: $H_2/nH = 14.0$, $H_2/MCP = 15.5$, $H_2/TeMB = 44$. With these conditions of reaction the catalytic activity was stable as a function of time on stream.

Activities are expressed as turnover numbers (TON), or number of molecules of reactant converted per surface metal atom and per hour. Selectivities are defined as $S_i = 100C_i/\sum_1^n C_j$, where C_i is the molar concentration of the produced alkane having i carbon atoms, while n is the total number of carbon atoms in the reactant. Selectivities were measured at low conversions, usually less than 5%, in order to avoid secondary reactions. They thus represent initial selectivities. Hydrogenolysis of an alkane on rhodium in these conditions is a simple reaction, with a single splitting of a C–C bond. The fragmentation factors ($\xi = \sum_1^{n-1} C_i/[\sum_1^{n-1}(i/n)C_i]$) defined following Paal and Tetenyi[34] are close to 2, except for large particles on which multiple fragmentations ($\xi > 2$) can occur.

Computational Methods

The LCGTO-MP-LSD method has been described in refs 28 and 29. The VWN local spin density potential has been used.[35] For the Rh atom, the 4p electrons were included in the valence shell, whereas only the (4s, 4p) electrons for germanium and (5s, 5p) electrons for tin were treated as valence electrons. For all atoms, the core electrons were replaced by model potentials.[28,36] The patterns of the orbital basis sets used in the computation for Rh, Ge, and Sn are (2211/2111/11*), (311/2111/1*), and (221/2111/1*), respectively, where numbers in parentheses denote the size of the contraction and slashes separate different symmetries (with * for polarization and + for diffuse functions). The orbital and auxiliary basis sets and model potentials have been taken from ref 37 and 38. For all model clusters, a value of 0.269 nm has been adopted for the Rh–Rh distance. Two series of calculations have been performed. The first one concerns $Rh_{10}M_4$ (I, C_{2v}) and $Rh_{10}M_3$ (II, C_{3v}) being models of the (100) and (111) faces, respectively (Figures 1 and 2).

(30) Kip, B. J.; Hermans, E. G. F.; Prins, R. *Proceedings 9th International Congress Catalysis*, Calgary, 1988; Chemical Institute of Canada: Ottawa, 1988; Vol. 2, p 821.
(31) Nunez, G. M.; Patrignani, A. R.; Rouco, A. J. *J. Catal.* **1986**, *98*, 554.
(32) Coq, B.; Figueras, F.; Tazi, T. *Z. Phys. D* **1989**, *12*, 579. Coq, B.; Dutartre, R.; Figueras, F.; Tazi, T. *J. Catal.* **1990**, *122*, 438.
(33) Kip, B. J.; Duivenvoorden, F. R. M.; Koningsberger, D. C.; Prins, R. *J. Catal.* **1987**, *105*, 26.
(34) Paal, Z.; Tetenyi, P. *Nature (London)* **1977**, *267*, 234.
(35) Vosko, S. H.; Wilk, L.; Nusair, N. *Can. J. Phys.* **1980**, *58*, 1200.
(36) Sakai, Y.; Husinaga, S. *J. Chem. Phys.* **1982**, *76*, 2537, 2552.
(37) Andzelm, J.; Russo, N.; Salahub, D. R. *J. Chem. Phys.* **1987**, *87*, 6562.
(38) Rochefort, A. M. Sc. Thesis, Université de Montréal, 1989.

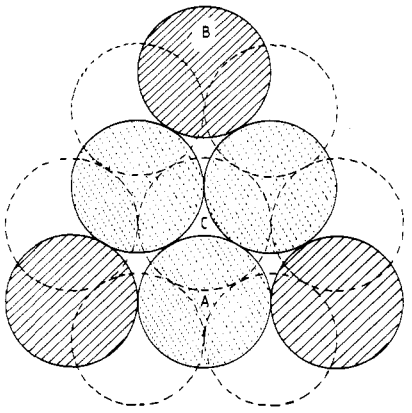

Figure 2. Model cluster of the (111) face of $Rh_{10}M_3$ and $Rh_{12}M$ (M in A, B, C sites): solid lines, 1st layer; dashed lines, 2nd layer; hachered spheres, Sn and Ge atoms in low coordination sites (N = 4), $Rh_{10}M_3$; dotted spheres, Sn and Ge atoms in high coordination sites (N = 7), $Rh_{10}M_3$.

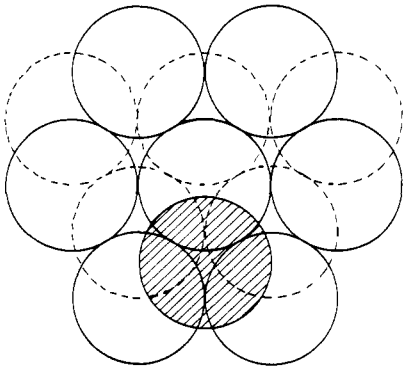

Figure 3. $Rh_{12}M$ model cluster with M adsorbed on a 3-fold hollow site: 1st layer, solid lines; 2nd layer, dashed lines; the hachered sphere represents the M atom adsorbed on the 1st layer.

The number of Sn and Ge atoms has been chosen in order to be consistent with the experimental M/Rh ratios and also to keep the indicated symmetry. For each model cluster, the M atoms are positioned either in low (1a, 11a) or in high (1b, 11b) coordination sites. The M–M distances have been optimized for $Rh_{10}M_4$ with the M atoms in both the low and high coordination sites (Figure 1). This optimization has been performed with the assumption that Rh–M = 0.5(Rh–Rh + M–M). The same optimal Sn–Sn (0.28 nm) and Ge–Ge (0.27 nm) bond distances have been obtained, whichever were the sites occupied by the Sn or Ge atoms. These M–M bond distances have then been used for $Rh_{10}M_3$.

The second series of calculations involves $Rh_{12}M$, model clusters of the (111) face. Their relative stabilities have been compared when M is an edge, corner, or in-plane atom (Figure 2, M in A, B, C, respectively) and when it is moved to a 3-fold hollow site, as if it was chemisorbed (Figure 3). The Rh–M distance has been optimized for $Rh_{12}M$. This optimization led to Rh–M distances (Rh is the first nearest neighbor) of 0.240 nm for Ge and 0.265 nm for Sn, where M was a corner atom (111b) or a chemisorbed one (111d).

In most calculations, performed with the standard LCGTO-LSD programs, an angular mesh consisting of 12 points is used for the sampling of the exchange correlation potential. Some recent tests on small systems[39] have shown that this grid may be inadequate for comparisons of small energy differences between structures where some atoms are moved in a fashion that changes their positions relative to the grid points. We have therefore repeated some of the calculations with a 62-point angular grid, which yielded rotational invariance on test molecules (PdH, Pd_2H) to within 0.015 eV. Our test involving $Rh_{10}Ge_4$ led to a difference of 6 kcal/mol for E(1a) – E(1b) (see Table VII) between the calculations performed with the 62-point and the 12-point grids. This difference amounted to 10 kcal/mol for $Rh_{12}Ge$, E(111b) – E(111d) (see Table VIII). The 12-point grid has therefore induced an uncertainty in the relative energies (Tables VII and VIII) of about this order of magnitude. For the present clusters, the orientations chosen for the tests were very different so that the estimate of the uncertainty is realistic. Then, in the following we treat energy differences of less than 10 kcal/mol as lying within the "errors bars" of our calculations.

(39) Andzelm, J.; Mijoule, C.; Papai, I.; Saint-Amant, A. Unpublished results.

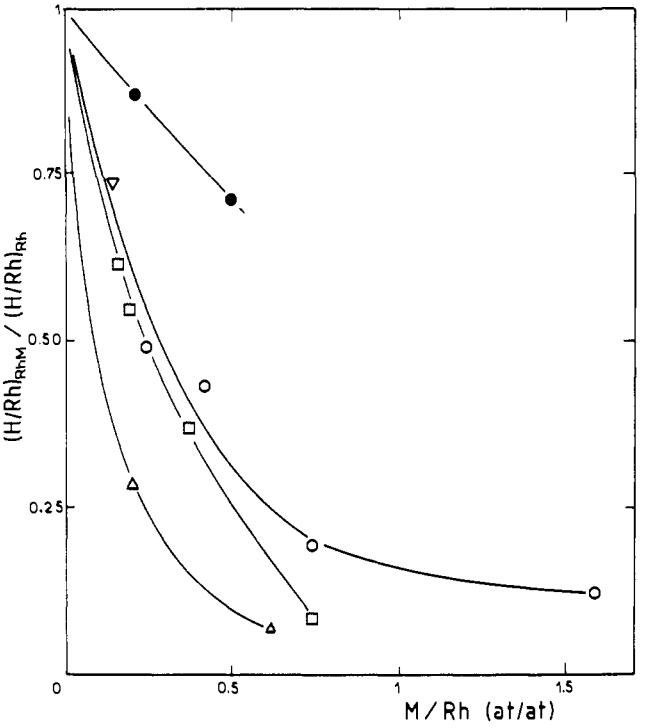

Figure 4. Hydrogen uptake (normalized to hydrogen uptake on the pure Rh/Al_2O_3 parent catalyst) as a function of the amount of second metal M in RhM/Al_2O_3 catalysts; (●) RAl2Sn, (○) RAl6Sn, (□) RAl8Pb, (△) RAl8Ge, (▽) RAl8Sb.

Results of Catalysis

The use of $Rh(acac)_3$ as a precursor allowed the preparation of Rh/Al_2O_3 catalysts with a wide range of metal dispersion (Table I), without introducing chlorine which can modify both chemisorption and catalytic properties.[32] The occurrence of H/Rh > 1 is now well established for Rh particles smaller than 1 nm and was interpreted as multiple adsorption of hydrogen on one surface Rh atom.[33,40] The modification of a parent Rh/Al_2O_3 sample, with $Sn(C_4H_9)_4$ for instance, leads to well-defined $RhSn/Al_2O_3$ catalysts. In the range of metal compositions studied, the addition of Sn, or another second metal, produces an increase of particle size corresponding merely to the added volume of this second metal. The subsequent reduction of $RhSn(C_4H_9)_x/Al_2O_3$ at 673 K does not induce a sintering of the bimetallic particles. This behavior confirms previous reports on RhSn,[8] RuM,[10] and PdM[7] catalysts.

Figure 4 reports the hydrogen chemisorption as a function of the amount of the second metal in RhM/Al_2O_3 catalysts. The amounts adsorbed were normalized with respect to the uptake on the parent Rh/Al_2O_3 catalyst. It appears that the following are observed: (1) The decrease of hydrogen uptake upon similar Sn addition is lower on very small aggregates (dp < 1 nm). (2) At similar particle sizes (RAl6 and RAl8 based catalysts, dp ~ 1.3–1.4 nm), the hydrogen chemisorption falls in the same curve for small amounts of Sn, Pb, or Sb added (M/Rh < 0.5 atom/atom). High tin addition (Sn/Rh = 1.6) reproduces the same decrease of chemisorption as reported elsewhere for RuM/Al_2O_3 catalysts.[10] (3) With respect to the previous point, the effect of Ge differs, since the decrease in H_2 chemisorption is larger.

Before presenting the effect of the second metal on catalytic properties of rhodium for the hydrogenolysis of alkanes, it is necessary to recall some aspects of the dependency of these reactions on Rh particle size:[32] (1) When going from large to small

(40) Crucq, A.; Degols, L.; Frennet, A.; Lienard, G. *Catal. Today* **1989**, *5*, 223.

Table III. Catalytic Properties of Rh/Al_2O_3 Catalysts for the Conversion of 2,2,3,3-Tetramethylbutane at 493 K (from Ref 32)

catalysts	H/Rh	conv, %	TON, h^{-1}	product distribution, % C_1	iC_4	TrMB[a]	E_a, kJ/mol
RAl5	0.08	2.6	33	5.9	91.5	2.6	59
RAl3	0.35	4.5	20	4.7	91.4	3.9	59
RAl8	0.74	5.0	24	11.6	78.7	9.7	59
RAl6	0.90	4.2	7.6	16.6	68.0	15.4	58.5
RAl2	1.0	3.5	6.5	44.2	16.3	39.5	46
RAl2D	1.7	3.3	12	52.8	4.7	45.9	44.5

[a] TrMB = 2,2,3-trimcthylbutane.

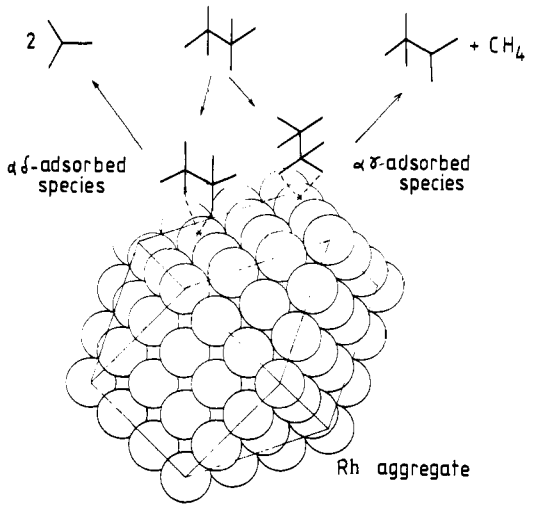

Figure 5. Schematic representation of the two pathways for TeMB hydrogenolysis on a supported Rh aggregate (the asterisk refers to the active site which can be one or several metal atoms).

particles the specific activity increased from 60 to 240 h^{-1} for nH conversion but decreased from 400 to 70 h^{-1} for MCP ring opening. (2) Large particles favor demethylation of nH and selective ring opening of MCP to 2-methyl- and 3-methylpentane. Small particles favor internal cleavage of nH and a less selective ring opening of MCP (small formation of nH).

In other respects the most significant changes were observed when converting TeMB. Table III reports the main features of TeMB hydrogenolysis on Rh/Al_2O_3 catalysts of varying dispersions, which can be summarized as the following: (1) On large Rh particles (dp > 4 nm) a selective splitting between the two quaternary carbon atoms leads to isobutane (iC_4). This central cleavage of TeMB occurs by means of $\alpha\delta$-adsorbed species (Figure 5), as shown by D_2/TeMB exchange.[21] However, we noticed that activation energy for D_2/TeMB exchange ($\alpha\delta$ formation) is well below that for hydrogenolysis, 20 compared to 59 kcal/mol. (2) On small Rh particles (dp < 1 nm) the preferred route for TeMB hydrogenolysis is demethylation to 2,2,3-trimethylbutane and methane, through $\alpha\gamma$-adsorbed species (Figure 5). As recognized by Brown et al.,[21] the ability to form $\alpha\gamma$ and $\alpha\delta$ intermediates with TeMB is the main characteristic of rhodium. (3) Finally we have noticed that TON does not change so much (20 ± 10 h^{-1}) with Rh/Al_2O_3 prepared from $Rh(acac)_3$. This behavior differs totally for Rh/Al_2O_3 issuing from $RhCl_3 \cdot 3H_2O$ for which TON decreased by 10^3 with increasing dispersion.[32]

Moving back now to the bimetallic RhM/Al_2O_3 catalysts, Figure 6 reports, with respect to the pure Rh/Al_2O_3 sample, the TON for nH hydrogenolysis as a function of the second metal content. The effect of Sn, Pb, or Sb on TON is nearly the same: at low second metal content the change of activity is small, but it decreases sharply when M/Rh > 0.5. At variance with this, a small addition of Ge decreases the TON by an order of magnitude. These effects are general rules for MCP and TeMB hydrogenolysis.

Moreover, the second metal modifies also the direction for hydrogenolysis. Tables IV–VI report the modification patterns

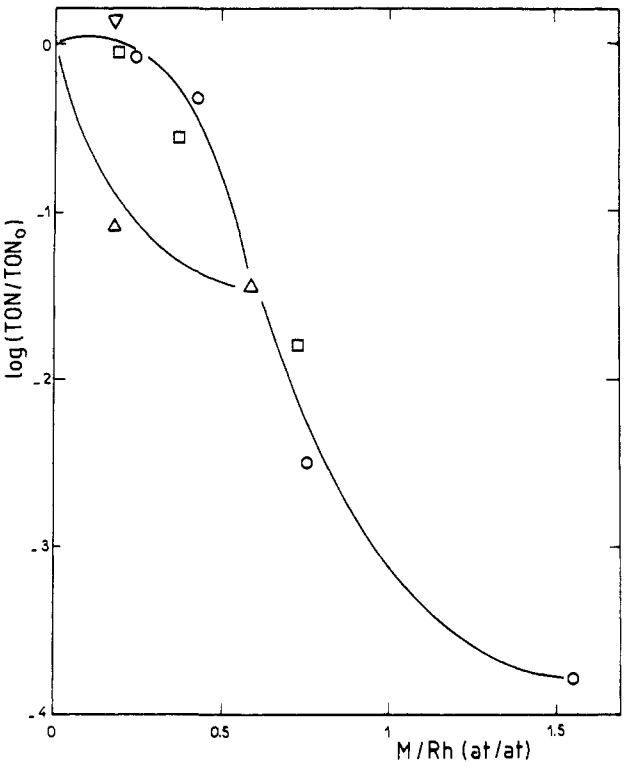

Figure 6. Relative specific activity of RhM/Al_2O_3 to that of the parent Rh/Al_2O_3 as a function of content of the second metal for the hydrogenolysis of *n*-hexane; same symbols as in Figure 4.

Table IV. Influence of the Dispersion of the Rh/Al_2O_3 Parent Sample on the Catalytic Properties of $RhSn/Al_2O_3$ Catalysts for the Conversion of 2,2,3,3-Tetramethylbutane at 493 K

catalysts	wt % of Sn	conv, %	TON, h^{-1}	product distribution, % C_1	iC_4	TrMB
RAl6	0	4.2	7.6	16.6	68	15.4
RAl6Sn1	0.2	1.5	7.2	13.7	73.1	13.2
RAl6Sn2	0.43	0.6	3.3	13.5	73.0	13.5
RAl6Sn3	0.75	1.5	0.01	10.0	80.5	9.5
RAl2	0	3.5	6.5	44.2	16.3	39.5
RAl2Sn2	0.21	0.6	2.1	45.7	5.8	48.5
RAl2Sn3	0.50	0.4	0.6	44.1	7.1	48.8

[a] From RAl6 sample (H/Rh = 0.9). [b] From RAl8 sample (H/Rh = 0.74).

Table V. Catalytic Properties of RhM/Al_2O_3 Catalysts (M = Pb, Sb, Ge) for the Conversion of 2,2,3,3-Tetramethylbutane at 493 K (Catalysts Prepared from the RAl8 Parent Sample, H/Rh = 0.74)

catalysts	wt % of M	conv, %	TON, h^{-1}	product distribution, % C_1	iC_4	TrMB
RAl8	0	5.0	24	11.6	78.7	9.7
RAl8Pb2	0.19	1.7	10.2	8.5	84.4	7.0
RAl8Pb3	0.37	3.3	4	7.2	86.2	6.6
RAl8Pb1	0.73	2.4	0.1	8.8	87.6	3.5
RAl8Sb	0.19	4.9	37.2	11.7	78.5	9.7
RAl8Ge1	0.20	0.20	0.21	18.5	66.8	14.7
RAl8Ge2	0.70	0.30	0.08	39.2	22.9	37.9

Table VI. Catalytic Properties of $RhPb/Al_2O_3$ and $RhGe/Al_2O_3$ Catalysts for the Conversion of *n*-Hexane and Methylcyclopentane at 493 K (Catalysts Prepared from RAl8)

	product distribution in nH conversion, %					product distribution in MCP conversion, %			
catalysts	C_1	C_2	C_3	nC_4	nC_5	$<C_6$	2MP	3MP	nH
RAl8	23.0	21.0	21.0	19.6	13.4	6.2	65.1	24.1	3.6
RAl8Pb3	23.3	20.9	20.7	19.9	14.9	3.7	71.1	24.0	1.1
RAl8Ge2	17.7	21.2	26.4	20.1	13.9	6.5	55.6	28.1	9.6

Table VII. Relative Energies (kcal/mol) of $Rh_{10}M_3$ (C_{3v}) and $Rh_{10}M_4$ (C_{2v}) Model Clusters

model	coord no. of M site	no. of M–M bonds[a]	rel energies, kcal/mol
$Rh_{10}Sn_4$, Ia	4	2	0
$Rh_{10}Sn_4$, Ib	8	6	130
$Rh_{10}Ge_4$, Ia	4	2	0
$Rh_{10}Ge_4$, Ib	8	6	91[b]
$Rh_{10}Sn_3$, IIa	4	0	0
$Rh_{10}Sn_3$, IIb	7	3	164
$Rh_{10}Ge_3$, IIa	4	0	0
$Rh_{10}Ge_3$, IIb	7	3	71

[a] Calculations performed with the following values: Sn–Sn = 0.280 nm; Sn–Rh = 0.274 nm; Ge–Ge = Ge–Rh = Rh–Rh = 0.269 nm. [b] 97 kcal/mol with the 62 grid points.

for nH, MCP, and TeMB hydrogenolysis, when adding Sn, Pb, Sb, and Ge to a Rh/Al_2O_3 parent catalyst.

On catalysts prepared from Rh/Al_2O_3 with similar Rh particle size (RAl6 and RAl8, dp = 1.3–1.5 nm), the addition of Sn or Pb favors the $\alpha\delta$ process to iC4 in TeMB conversion. In the absence of any significant change of the metallic particle size, the selectivity pattern of larger Rh particles (dp > 3 nm) is thus reproduced. On very small aggregates (RAl2D based catalyst) the effect of Sn addition is much less sensitive and the $\alpha\delta$ process is little increased. On the other hand, adding Ge to RAl8 catalyst favors clearly the $\alpha\gamma$ process, and properties looking like those of smaller Rh particles are obtained. The effect of Sb on the properties of rhodium for hydrogenolysis is intermediate between that of Sn, Pb and of Ge. These facts indicate that adding Sn, Pb, Sb, or Ge does not reproduce the same behavior as expected from the ensemble theory of alloys.

Finally, the changes of catalytic properties are more or less pronounced depending on the reaction studied as a catalytic probe. The addition of Pb decreases the ring opening of MCP to nH, whereas adding Ge favors this last reaction and the internal cleavage of nH to propane as well. The changes of nH and MCP selectivity patterns upon Pb and Ge addition to the RAl8 catalyst are in agreement with the considerations derived before from TeMB hydrogenolysis. However, these modifications of catalytic properties are less pronounced than in this last reaction.

Results from Calculations

First of all, let us recall that the real aggregates, whose size is less than 1 nm, lead to only one type of C–C bond cleavage (i.e. TeMB converted to methane and 2,2,3-trimethylbutane), since they do not contain planes with highly coordinated atoms. Then, the presence of a second metal does not change the catalysis. It is only for 1.2–1.5 nm aggregates that the two different routes for TeMB decomposition exist, with an observed influence of the addition of a second metal. It is worth noting that the smallest perfect cuboctahedral particle, having only one atom in the middle of a (100) face, already contains 55 atoms.

The models we have chosen are, of course, much smaller than the real particles. We believe, however, that they are sufficiently large and well chosen to allow reliable comparisons of the behaviors of RhSn and RhGe clusters, with respect to the sites occupied by Sn and Ge atoms. It would, of course, be reassuring to be able to add further shells of atoms or, indeed, to study more examples of geometric arrangements; however, the present calculations, which already represent a sizable investment in computer time (about 4.7 h on a Cray XMP for one geometry), provide valid insight on a number of questions raised by the experimental work.

(1) $Rh_{10}M_4$ and $Rh_{10}M_3$ Models (M = Ge, Sn). The first point we wanted to clarify was to check if, for an experimental M/Rh ratio, the calculations would support the "observed" trend of Sn atoms to segregate essentially into low coordination sites, and also the conclusion that Ge atoms do not behave so exclusively. Both models describing the (100) and (111) faces have been studied, in order to eliminate symmetry and shape effects. The results of these calculations are presented in Table VII. For both C_{2v} and C_{3v} symmetries, the clusters (Ia, IIa) with Sn or Ge atoms in low coordination sites are the most stable. However, it is obvious that tin atoms have a greater tendency to occupy corner sites than have germanium atoms, since the related RhSn clusters are much more stabilized (130 and 160 kcal/mol) than the RhGe ones (91 and 71 kcal/mol). This trend, exhibited by RhSn models, does not seem to be correlated with some greater repulsion between Sn atoms. Indeed, the energy difference E(Ia) – E(Ib) is smaller than E(IIa) – E(IIb), although Ib has 4 more Sn–Sn bonds than Ia, versus 3 more for IIb with respect to IIa.

Table VIII. Relative Stabilities (kcal/mol) of $Rh_{12}Ge$ and $Rh_{12}Sn$ Models, When Different Sites Are Occupied by Ge and Sn

compd	site	coord no.	rel energies, kcal/mol	
			$Rh_{12}Ge$	$Rh_{12}Sn$
IIIa	edge	7	17	45
IIIb	corner	4	0	0
IIIc	center of face	9	40	57
IIId	chemisorbed	3	16	31

On the contrary, for RhGe clusters, the preferred occupancy of corner sites can be related to the smaller number of Ge–Ge pairs, as suggested by the ordering of the energy differences E(Ia) – E(Ib) > E(IIa) – E(IIb), correlated with additional Ge–Ge interactions. These conclusions are confirmed by the values obtained for the optimized M–M bonds, in the case of cluster I: the Sn–Sn distance for Ia and Ib is 0.28 nm, in agreement with the Sn–Sn bond distance in the bulk, and the calculated value in the dimer (0.273 nm[37] or 0.275 nm[41]). However, although Ge–Ge bonds are 0.245 nm in the bulk and calculated at 0.238 nm[37] or 0.242 nm[42] for the dimer, this value does not correspond to the lowest energy for the RhGe clusters (obtained for 0.270 nm). One can thus conclude that, in the presence of Rh atoms, the Ge atoms have a tendency to disperse in the Rh lattice, rather than making Ge–Ge bonds.

The representation of 3 or 4 M atoms in our RhM models is necessarily approximate, especially for in-plane M atoms, and the calculated relative energies are therefore only indicative. However, these results do show that Sn segregation into low coordination sites is more favored than that for Ge atoms, and that the distribution of this latter metal in the cluster is accompanied by a tendency to avoid Ge–Ge bonds.

In order to investigate in more detail the incidence of the sites occupied by the second metal on the cluster stability, we have performed another series of calculations on the model cluster II, containing only one Ge(Sn) atom.

(2) $Rh_{12}M$ Models (M = Ge, Sn). In a first step, the $Rh_{12}Ge$ cluster has been extensively studied, with optimization of the Rh–Ge distances, for each typical position of the Ge atom: edge, corner, center of face, and "chemisorbed" position. These respective locations of the Ge atom are indicated as A, B, and C in Figure 2 and A in Figure 3. The model cluster of the (111) face has been chosen for this study, since it allowed comparisons of the relative stabilities for all models containing one Ge(Sn) atom, in the different sites, while keeping the same C_s symmetry. The distances between a chemisorbed or a corner Ge atom and the nearest Rh neighbors have the same optimized value of 0.240 nm. In both cases, the variations of the total energies with this distance were very similar, and the energy gain with respect to a value of 0.269 nm was about 18 kcal/mol. This optimized bond distance for the two other models (edge and face sites) has a common value close to 0.260 nm, the nearest Rh atoms being, in each case, the nearest 3 equivalent atoms of the layer without Ge (2nd layer for Ge in A, 1st layer for Ge in C, Figure 2). But, for these models, the stabilization with respect to the Rh lattice (0.269 nm) is found to be very small (2 kcal/mol). It should be borne in mind that the above relaxation effects are calculated for a very small cluster model; relaxation in the real catalytic particles might be significantly different and the above values should be taken as only indicative.

(41) Balasubramanian, K.; Pitzer, K. S. *J. Chem. Phys.* **1983**, *78*, 321.
(42) Shim, I.; Nagarathra-Naik, H. M.; Gingerich, K. A. *Int. J. Quantum Chem.* **1986**, *29*, 975.

The results obtained for $Rh_{12}Ge$ (Table VIII) suggest the following: (a) The corner site is the most favored one. However, the edge and chemisorbed sites are not too much higher and could remain possible locations for Ge, especially if one keeps in mind the 10 kcal/mol uncertainty related to the use of 12 grid points and the other uncertainties of the model. (b) The replacement of a Rh by a Ge atom in the middle of a face is far less favorable than this replacement in a corner or edge site.

In light of the results obtained from the optimizations of the Rh–Ge distances, the Rh–Sn distance has been optimized for $Rh_{12}Sn$ models, only when Sn occupies a corner or a chemisorbed position. The optimized Rh–Sn distances were then 0.265 nm.

For a Sn atom in edge or face sites, a fixed Rh–Sn distance of 0.280 nm has been used. The possible error related to this choice is assumed to lie within the previously reported 10 kcal/mol uncertainty.

The results obtained for $Rh_{12}Sn$ (Table VIII) show that the corner site is, by far, the most stable one, all the other possibilities being energetically unfavored. The comparison between $Rh_{12}Ge$ and $Rh_{12}Sn$ shows, without doubt, that Sn will segregate essentially to the corners, while Ge does not have such a definite preference.

It is worth noting that the stabilities of these RhM clusters are not directly dependent on the coordination number of the M site. Indeed, the three "possible" sites for Ge have variable coordination numbers (3, 4, 6), and the preferred site for Sn (corner) is not the least coordinated. Moreover, a chemisorbed Sn atom, which has the smallest number of Rh first neighbors, corresponds to a very unfavorable case.

Examination of the molecular orbitals (MOs) of these clusters shows that there is some correlation between their stabilities and the energies of the 20 a′ Rh–M bonding MO. For the RhGe clusters, this MO, which is responsible for the major bonding interactions between Ge 4s and Rh 5s orbitals, has relatively comparable energies for the edge, corner, and chemisorbed Ge positions (−13.30, −13.50, and −13.20 eV, respectively), with respective contributions of 70%, 65%, and 62% of the Ge 4s orbital. Moreover, the greater stability of this MO in the corner case (−13.50 eV) is compensated by three less stable MOs at −7.19, −7.10, and −7.07 eV, instead of −7.31, −7.21, and −7.20 eV for the chemisorbed site. These MOs, 33 a′, 25 a″, and 34 a′ respectively, are complex combinations of bonding and antibonding Rh 4d–Rh 4d and Rh 5s,4d–Ge 4s,4p interactions.

In the case of an isolated Sn atom, the Sn 5s orbital is about 1.3 eV less stable than the Ge 4s orbital (see calculated ionization energies in ref 37). A comparable energy gap appears between the 1 σ_g MOs of the Ge_2 and Sn_2 dimers,[37] while the difference is reduced to about 1.0 eV between the related 10 σ_g MOs of the PdGe and PdSn diatomics.[43] In agreement with these results, the Rh 5s–Sn 5s bonding MOs of the $Rh_{12}Sn$ models appear about 1.1–1.2 eV higher in energy than the Rh 5s–Ge 4s MOs of the corresponding $Rh_{12}Ge$ clusters.

It is not obvious that a definite correlation between the electronic structures of the different $Rh_{12}Sn$ models and their relative stabilities can be drawn. The greater stability of the corner model, especially with respect to the adsorbed Sn structure, is a balance of more stable/less stable Rh–Sn interactions. As was the case for the RhGe clusters, the 20 a′ MO is responsible for the major Rh–Sn bonding. Again, this MO is more stable in the corner case (−12.47 eV) than in the adsorbed Sn model (−12.10 eV). Indeed, in comparing the RhSn results with those for RhGe, one can see that the differences in orbital energies reflect the differences in total energies to a reasonable extent. Analysis of the orbitals shows that for the corner case, there are four strong bonding interactions between Sn 5s (60%) and the 5s orbitals of the four nearest Rh neighbors, while for the chemisorbed case, the Sn 5s orbital (70%) has a positive overlap with only two Rh neighbors.

For both RhGe and RhSn models, the variations of the more or less bonding Rh–M contributions according to the M site are rather complicated, with even a non-negligible incidence on the Rh 4p orbital energies, which have been treated as valence orbitals.

Table IX. Mulliken Analysis for $Rh_{12}M$ and $Rh_{10}M_4$ Models

model	site	total charge, electrons	
		Ge	Sn
$Rh_{12}M$	IIIa edge	3.85	3.60
	IIIb corner	4.22	3.45
	IIId chemisorbed	3.74	3.43
$Rh_{10}M_4$	Ia	3.77	3.62
	Ib	3.65	3.20

Mulliken analyses (Table IX) have been performed. The net charge calculated on each M atom varies with the site and the Rh–M distance. However, the Sn atoms are always found to bear a positive net charge, 0.2 to 0.4 larger than the net charge calculated on the related Ge atoms. This means that, whichever are the sites they occupy, Sn atoms donate electrons to Rh and Ge atoms are always more electronegative than Sn. The calculated net charge on Ge has been found to be negative (−0.2) only in the case of IIIb, with Ge in a corner. These results are consistent with the trends calculated for the diatomics GeSi, SnSi, and GeSn,[37] where Ge was found to be more electronegative than Sn. This result is in agreement with Pauling's electronegativity order (2.01 for Ge and 1.96 for Sn). In the case of PdSn and PdGe, the calculated net charges were opposite, negative on Ge and positive on Sn.[43] Notwithstanding the well-known limitations of this charge analysis scheme, the following comparisons should be valid.

Discussion

The data for alkane conversion show changes in catalytic properties upon adding a second component to pure rhodium alumina catalysts. These changes are the most pronounced when the following conditions exist: (a) the rhodium particles range in size between 1 and 1.5 nm (RA16 and RA18 based samples) [For these cluster sizes, the number of atoms located either on the faces or the edges and corners are balanced. In contrast to this, the very small aggregates of the RA12D sample (dp < 1 nm) only contain edge and corner atoms.] (b) Lead, tin, or germanium are added to rhodium. (The addition of antimony has little effect.) (c) The hydrogenolysis of TeMB is considered. (As for the effect of Rh particle size, the sensitivity of nH and MCP hydrogenolysis to Rh alloying is lower.)

Summing up these considerations the main feature appearing is that the addition of Pb or Sn on Rh/Al_2O_3 mimics the properties of larger Rh clusters, but the reverse is true when Ge is added. The shift of properties of Rh particles toward those of larger size upon Pb or Sn addition cannot be explained by the ensemble theory of alloys. Indeed, this model predicts a shift of the properties in the direction of smaller particles upon the addition of an inactive component to the metallic surface, as reported for NiCu alloys.[44]

We proposed previously that edge and corner atoms of Rh particles are responsible for the $\alpha\gamma$ process, leading to demethylation of TeMB. The disappearance of this process upon Sn and Pb addition on RA18 or RA16 samples can be understood, assuming a topological segregation of Sn or Pb to the surface of RhM bimetallic particles. In this model, an ordered layer on RhSn and RhPb clusters exists, in which Sn and Pb atoms occupy corner and edge sites. Very likely, large islands of Rh atoms remain free on the facets, since the TON for alkane hydrogenolysis does not decrease significantly for a low amount of the second component (M/Rh < 0.4). The situation is different for RhGe clusters where germanium could be randomly distributed. The subsequent dilution of the active Rh surface decreases the TON and mimics the selectivity of smaller Rh clusters. Obviously, these effects are obscured when tin is added on Rh clusters containing only corner or edge atoms (RA12D based catalysts).

The classical physical reasons invoked to explain surface segregation of the second metal in bimetallic alloys could be applied to understand site segregation: the component which segregates

(43) Russo, N.; Andzelm, J.; Salahub, D. R. *Chem. Phys.* **1987**, *114*, 331.

(44) Roberti, A.; Ponec, V.; Sachtler, W. M. H. *J. Catal.* **1973**, *28*, 381.

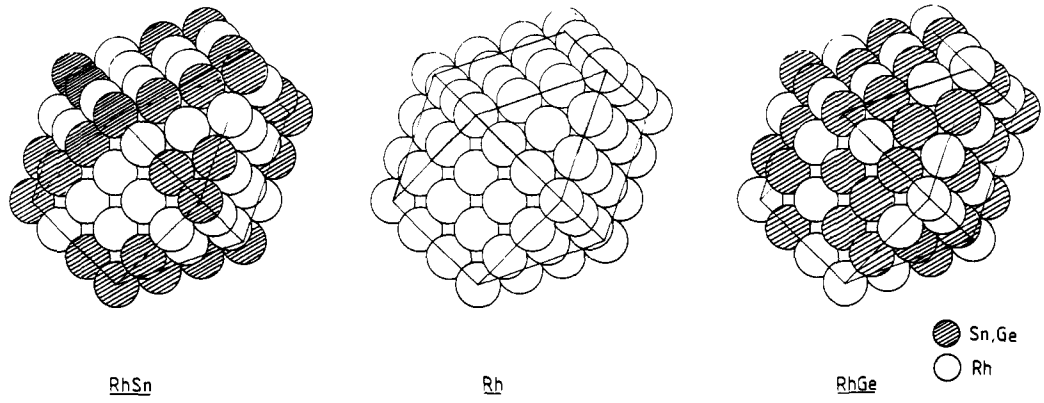

Figure 7. Model clusters of bimetallic RhSn and RhGe (Sn,Ge/Rh = 0.2, atom/atom) with a perfect cubooctahedral habit; the total number of atoms is 147.

at the surface has either the lowest heat of sublimation[12] or the largest atomic radius.[13] Both reasons lead to segregation of Sn, Pb, or Sb atoms to the surface and could account for a preferential location of these elements at corner or edge sites of Rh bimetallic particles. However, they are conflicting for Ge atoms (lower heat of sublimation but lower atomic radius than rhodium). In fact, this inconsistency shows that simple (thermodynamic) models seem inadequate to predict the site segregation phenomenon.

In spite of the uncertainties on the calculated total energies, due to the restricted size of the model clusters and to the limitations inherent to the quantum chemical calculations (see computational details), our theoretical approach has given a picture of Sn and Ge segregation which is consistent with our experimental results. Indeed, it has shown that Sn atoms will preferentially be distributed in the lowest coordination sites of Rh particles, with the exception of sites of chemisorption. This is proved by the unambiguously greater stability of the models containing Sn atoms at the periphery of the cluster, i.e. $Rh_{10}Sn_4$ (Ia), $Rh_{10}Sn_3$ (IIa), and $Rh_{12}Sn$ (IIIb). As far as substitution of Rh atoms is concerned, it should proceed first by corner atoms. Corner Sn atoms can also be created by building steps on the Rh surface. The preliminary replacement of highly coordinated atoms (N = 7, 9, Table VIII) is shown to be energetically very unfavored. Moreover, in spite of the low coordination of the site, the adsorption of a Sn atom on a Rh face does not correspond to a stable situation. This result could be indicative of a preferred direct substitution of Rh by Sn atoms. If additional amounts of Sn are then introduced in the same Rh base catalyst (for example RAl6), Sn atoms have no choice and must occupy the dense planes of the particle. The classical phenomenon of dilution of the surface is then observed with a sharp decrease of hydrogenolysis activity (RAlSn4). A similar dilution of the Rh surface in $RhSn/Al_2O_3$ was also proposed by Candy et al.,[8] from the disappearance of the bridged CO band in IR spectroscopy.

In opposition to RhSn, the stabilities of RhGe clusters are shown to be less sensitive to the nature of the Ge sites.

The evaluated relative stabilities are consistent with clusters containing Ge atoms at corner or edge sites, and also distributed on Rh faces in 3-fold hollow sites, as if they were chemisorbed. Moreover, the results obtained for $Rh_{10}Ge_4$ (Ia, Ib) indicate that the germanium atoms tend to avoid Ge–Ge bonds, when they are in Rh clusters. These conclusions, derived from the calculations, are fully consistent with the picture of randomly distributed Ge atoms, as given by the experiments.

The main conclusions we have drawn, i.e. topological segregation of Sn and Pb to low coordination sites (ordered layer) and a random distribution of Ge (disordered layer), are illustrated in Figure 7. In the case of Sb, its behavior is intermediate between these two different types of distribution. These proposals are in agreement with our previous reports on RuM/Al_2O_3 catalysts.[10] In these supported bimetallic catalysts, Sn, Pb, or Sb segregate at corner and edge sites whereas Ge is also randomly distributed.

Finally, the calculated electron transfer from Sn to Rh, exhibited by all the models studied, is in agreement with the shift toward a lower frequency of the CO bond stretching observed in IR spectroscopy, for CO adsorbed on $RhSn/Al_2O_3$ catalysts.[8] The increase of the electronic density on Rh atoms should favor the back donation to antibonding π^* orbitals of the adsorbed CO molecule, and thus induce the weakening of the CO bond, followed by the lowering of its stretching frequency.

Acknowledgment. Financial support from the Natural Science and Engineering Research Council of Canada is gratefully acknowledged. The support of the France-Québec exchange program is highly appreciated as is the provision of computational resources from the Service Informatique de l'Université de Montréal, from NSERC, from Cray Canada and from the Centre National Universitaire Sud de Calcul de Montpellier. Peter Fillmore (Cray Canada) is thanked for his interest and support.

Registry No. MCP, 96-37-7; Rh, 7440-16-6; Sn, 7440-31-5; Pb, 7439-92-1; Sb, 7440-36-0; Ge, 7440-56-4; H_2, 1333-74-0; hexane, 110-54-3; 2,2,3-trimethylbutane, 464-06-2.